Pure Appl. Chem., Vol. 85, No. 1, pp. 115–133, 2013.
http://dx.doi.org/10.1351/PAC-CON-12-05-06

Fluids in random porous media: Scaled particle theory*

Myroslav Holovko[1,‡], Taras Patsahan[1], and Wei Dong[2]

[1]Institute for Condensed Matter Physics of the National Academy of Sciences of Ukraine, 1 Svientsitskii Str., 79011 Lviv, Ukraine; [2]École Normale Supérieure de Lyon, 46 Allée d'Italie, 69364 Lyon, Cedex 07, France

Abstract: The scaled particle theory (SPT) is applied to describe thermodynamic properties of a hard sphere (HS) fluid in random porous media. To this purpose, we extended the SPT2 approach, which has been developed previously. The analytical expressions for the chemical potential of an HS fluid in HS and overlapping hard sphere (OPH) matrices, sponge matrix, and hard convex body (HCB) matrix are obtained and analyzed. A series of new approximations for SPT2 are proposed. The grand canonical Monte Carlo (GGMC) simulations are performed to verify an accuracy of the SPT2 approach combined with the new approximations. A possibility of mapping between thermodynamic properties of an HS fluid in random porous media of different types is discussed. It is shown that thermodynamic properties of a fluid in the different matrices tend to be equal if the probe particle porosities and the specific surface pore areas of considered matrices are identical. The obtained results for an HS fluid in random porous media as reference systems are used to extend the van der Waals equation of state to the case of a simple fluid in random porous media. It is observed that a decrease of matrix porosity leads to lowering of the critical temperature and the critical density of a confined fluid, while an increase of a size of matrix particles causes an increase of these critical parameters.

Keywords: equation of state; fluids; Monte Carlo simulation; phase transition; porous medium; scaled particle theory (SPT).

INTRODUCTION

Fluids in porous media with pore sizes ranging from a few nanometers to hundreds of nanometers can undergo drastic modifications in their physical and chemical properties. The understanding and the prediction of such changes in fluids properties is highly required for many practical applications. Much theoretical effort has been devoted to a study of fluids in porous materials during the last two decades starting from pioneering work of Madden and Gland [1]. In this paper, a simple model for a fluid adsorption in a random porous medium was proposed. Within this model, a porous medium is presented by quenched configurations of randomly distributed matrix particles. The specific of description of fluids in such matrices is connected with the double quenched-annealed averages: the annealed average is taken over all fluid configurations and the additional quenched average should be taken over all realizations of the matrix. One standard approach to solve this problem is based on the replica method. Using the replica Ornstein–Zernike (ROZ) integral equations [1,2], the statistical mechanics approach

Pure Appl. Chem.* **85, 1–305 (2013). A collection of invited papers based on presentations at the 32nd International Conference on Solution Chemistry (ICSC-32), La Grande Motte, France, 28 August–2 September 2011.
‡Corresponding author

of liquid state was extended to a description of different fluids confined in random porous matrices [3,4], including the chemical reacting fluids adsorbed in porous media [5,6]. Despite a comprehensive study of a fluid in random matrices, no analytical result has been obtained using the integral equation approach even for a simple model like a hard sphere (HS) fluid in an HS matrix. The main complication in a description of such a model appears due to the absence of direct interaction between particles from different replicated copies of a fluid. As a result, the description of this model is equivalent to a study of an HS mixture with strongly non-additive diameters, for which it is very difficult to find a correct analytical result within the integral equation approach.

The first rather accurate analytical results for an HS fluid in HS and overlapping hard sphere (OHS) matrices were obtained quite recently [7–9] by extending the scaled particle theory (SPT) [10–12] to the case of an HS fluid confined in a random porous media. The SPT approach is based on a combination of the exact treatment of a point scaled particle in an HS fluid with the thermodynamical consideration of a finite size scaled particle. The exact results for a point scaled particle in an HS fluid in random porous media was obtained in [7]. However, the proposed approach named as SPT1 contains a subtle inconsistency appearing when a size of matrix particles is essentially larger than a size of fluid particles. Later, this inconsistency was eliminated in a new improved approach named as SPT2 [9]. The expressions obtained in SPT2 include two types of porosities. One of them is defined by a pure geometry of porous medium (geometrical porosity ϕ_0), and the second one is defined by the chemical potential of a fluid in the limit of infinite dilution (probe particle porosity ϕ). On the basis of the SPT2 approach, the approximation SPT2b was proposed and it reproduces the computer simulation data with a good accuracy at small and intermediate fluid densities. In [13] the obtained results were generalized for one-dimensional hard rod fluid and two-dimensional hard disk fluid in random porous media. We should note that the expressions obtained in SPT2 and SPT2b approximations have a divergence when a packing fraction of fluid reaches the value equal to the probe particle porosity. Consequently, the prediction of thermodynamic quantities at high densities of a fluid becomes wrong. An accuracy of SPT2 and SPT2b also decreases when fluid and matrix particles are of comparable sizes [9]. Recently, in the investigation of one-dimensional hard rod fluid in random porous media we proposed the new approximations SPT2b1, SPT2b2, and SPT2b3, which are free of the noted inconsistency [14]. It was shown that these new approximations improve essentially the accuracy of SPT prediction. We believe that such approximations will be correct also for three-dimensional HS fluid in porous media.

In this review we summarize our recent development of the SPT2 theory for the theoretical description of thermodynamic properties of an HS fluid confined in random porous media. In order to assess the different approximations in the SPT2 theory, we performed grand canonical Monte Carlo (GGMC) simulations [15]. We consider four types of porous media depicted by the corresponding models known from the literature as HS, OHS, sponge [16,17], and hard convex body (HCB) matrices. Three of these matrices schematically are presented in Fig. 1.

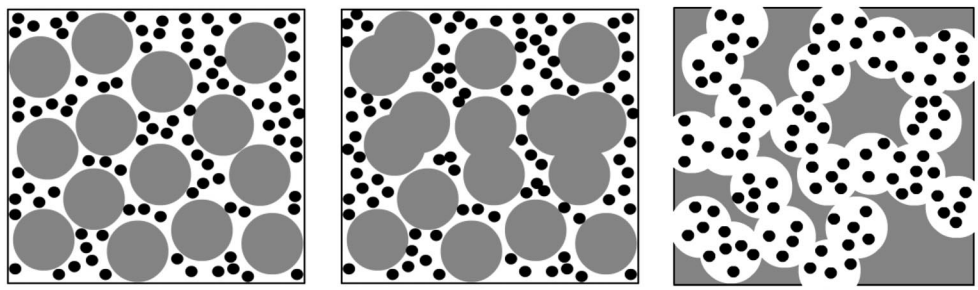

Fig. 1 Schematic presentations of the different models of porous medium: (a) HS matrix, (b) OHS matrix, (c) sponge matrix. Matrix particles are presented as large gray circles and fluid particles as black small circles.

The paper is organized as follows. A brief review of the SPT2 theory for an HS fluid in random porous media and computer simulations details are given in the beginning. Afterwards, the applications of the SPT2 theory for the description of an HS fluid in HS and OHS matrices, sponge matrix, and in a HCB matrix are presented. Next, the possibilities of mapping between the thermodynamic properties of HS fluid in porous media of different types are discussed. In the end, we consider the extension of the van der Waals equation of state for a simple fluid in random porous matrices.

SPT2 THEORY

The basic idea of the SPT is an insertion of an additional scaled particle of a variable size into a fluid. This procedure is equivalent to a creation of cavity, which is free of any other fluid particles. The key point of the SPT theory described in [7–14] consists of a derivation of the excess chemical potential of a scaled particle, μ_s^{ex}, which is equal to a work needed to create the corresponding cavity. In the presence of a porous medium the expression of excess chemical potential for a small scaled particle in an HS fluid is equal to [9]

$$\begin{aligned}\beta\mu_s^{ex} &= \beta\mu_s - \ln(\rho_1\Lambda_1^3) = -\ln\left[p_0(R_s) - \eta_1\left(1+\frac{R_s}{R_1}\right)^3\right] \\ &= -\ln p_0(R_s) - \ln\left[1 - \frac{\eta_1(1+R_s/R_1)^3}{p_0(R_s)}\right]\end{aligned} \tag{1}$$

where $\beta = 1/k_BT$, k_B is the Boltzmann constant, T is a temperature, R_s is the radius of scaled particle, R_1 is the radius of fluid particles, $\eta_1 = \frac{4}{3}\pi R_1^3\rho_1$ is the fluid packing fraction, ρ_1 is the fluid density, Λ_1 is the fluid thermal wavelength. The term $p_0(R_s) = e^{-\beta\mu_s^0}$ is defined by the excess chemical potential, μ_s^0, of the scaled particle confined in an empty matrix (limit of infinite dilution), and it has a meaning of probability to find a cavity created by this particle in the matrix in the absence of fluid particles. The term $p_{1/0}(R_s) = 1 - \frac{\eta_1(1+R_s/R_1)^3}{p_0(R_3)}$ is the probability to find a cavity created by the scaled particle in the fluid-matrix system under condition that the cavity is located entirely inside a pore occupied by the scaled particle.

For a large scaled particle ($R_s \geq 0$) the excess chemical potential, μ_s^{ex}, is given by a thermodynamic expression for the work needed to create a macroscopic cavity inside a fluid, and it can be presented in the following way:

$$\beta\mu_s^{ex} = w(R_s) + \beta P\frac{4}{3}\frac{\pi R_s^3}{p_0(R_s)} \tag{2}$$

where P is the pressure of fluid. It is worth noting that this expression has the same form as in the bulk case. A difference is only in the presence of multiplier term $1/p_0(R_s)$ in the last part. This multiplier appears due to an excluded volume occupied by matrix particles. For the bulk case, this multiplier is absent, since $p_0(R_s) = 1$. However, it was also erroneously skipped in the SPT1 theory [7] leading to the inconsistency discussed and corrected in [9], where $p_0(R_s)$ is considered as a probability to find a cavity created by the particle of radius $R_s \geq 0$ in the matrix in the absence of fluid particles. This probability is related directly to the different types of porosities of a matrix. First, when $R_s = R_1$

$$p_0(R_s = R_1) = e^{-\beta\mu_1^0} = \phi \tag{3}$$

one obtains the probe particle porosity, which is defined by the excess chemical potential of fluid particles in the limit of infinite dilution, μ_1^0, thus, it depends on the nature of a fluid under study. The second one is the geometrical porosity, which depends only on a structure of matrix and related to the volume of void existing between matrix particles, and it is defined as $p_0(R_s)$ in $R_s = 0$

$$p_0(R_s = 0) = \phi_0 \tag{4}$$

According to the ansatz of SPT [7–14], $w_s(R_s)$ can be presented in the form of expansion

$$w_s(R_s) = w_0 + w_1 R_s + \frac{1}{2} w_2 R_s^2 \tag{5}$$

The coefficients of this expansion can be found from the continuity of μ_s^{ex} and the corresponding derivatives $\frac{\partial \mu_s^{ex}}{\partial R_s}$ and $\frac{\partial^2 \mu_s^{ex}}{\partial R_s^2}$ at $R_s = 0$. As a result, one has [13]

$$\begin{aligned} w_0 &= -\ln(1-\eta_1/\phi_0) \\ w_1 &= \frac{\eta_1/\phi_0}{1-\eta_1/\phi_0}\left[\frac{3}{R_1} - \frac{p_0'}{\phi_0}\right] \\ w_2 &= \frac{\eta_1/\phi_0}{1-\eta_1/\phi_0}\left[\frac{6}{R_1^2} - \frac{6}{R_1}\frac{p_0'}{\phi_0} + 2\left(\frac{p_0'}{\phi_0}\right)^2 - \frac{p_0''}{\phi_0}\right] + \left(\frac{\eta_1/\phi_0}{1-\eta_1/\phi_0}\right)^2\left[\frac{3}{R_1} - \frac{p_0'}{\phi_0}\right]^2 \end{aligned} \tag{6}$$

where $p_0' = \frac{\partial p_0(R_s)}{\partial R_s}$ and $p_0'' = \frac{\partial^2 p_0(R_s)}{\partial R_s^2}$ at $R_s = 0$.

After setting $R_s = R_1$, the expression 2 gives the relation between pressure, P, and the excess chemical potential, μ_1^{ex}, of a fluid in a matrix:

$$\beta(\mu_1^{ex} - \mu_1^0) = -\ln(1-\eta_1/\phi_0) + A\frac{\eta_1/\phi_0}{1-\eta_1/\phi_0} + B\frac{(\eta_1/\phi_0)^2}{(1-\eta_1/\phi_0)^2} + \frac{\beta P}{\rho_1}\frac{\eta_1}{\phi} \tag{7}$$

where the constants A and B define the porous media structure and the expressions for them are

$$\begin{aligned} A &= 3 - \frac{p_0'}{\phi_0}R_1 + \frac{1}{2}\left[6 - 6\frac{p_0'}{\phi_0}R_1 + 2\left(\frac{p_0'}{\phi_0}\right)^2 R_1^2 - \frac{p_0''}{\phi_0}R_1^2\right] \\ B &= \frac{1}{2}\left(3 - \frac{p_0'}{\phi_0}R_1\right)^2 \end{aligned} \tag{8}$$

Using the Gibbs–Duhem equation

$$\left(\frac{\partial P}{\partial \rho_1}\right)_T = \rho_1\left(\frac{\partial \mu_1}{\partial \rho_1}\right)_T \tag{9}$$

one derives the compressibility in the following form:

$$\begin{aligned} \beta\left(\frac{\partial P}{\partial \rho_1}\right)_T &= \frac{1}{1-\eta_1/\phi} + (A+1)\frac{\eta_1/\phi_0}{(1-\eta_1/\phi)(1-\eta_1/\phi_0)} \\ &+ (A+2B)\frac{(\eta_1/\phi_0)^2}{(1-\eta_1/\phi)(1-\eta_1/\phi_0)^2} + 2B\frac{(\eta_1/\phi_0)^3}{(1-\eta_1/\phi)(1-\eta_1/\phi_0)^3} \end{aligned} \tag{10}$$

which makes it possible to obtain the total chemical potential, $\beta\mu_1 = \ln(\rho_1 {\Lambda_1}^3) + \beta\mu_1^{ex}$, as a result of integration of eq. 10 over the fluid density. Therefore, as it was shown previously in [9], the excess chemical potential can be derived [9]:

$$\begin{aligned}\beta(\mu_1^{ex}-\mu_1^0) &= -\ln(1-\eta_1/\phi)+(A+1)\frac{\phi}{\phi_0-\phi}\ln\frac{1-\eta_1/\phi}{1-\eta_1/\phi_0}\\ &+(A+2B)\frac{\phi}{\phi_0-\phi}\left(\frac{\eta_1/\phi_0}{1-\eta_1/\phi_0}-\frac{\phi}{\phi-\phi_0}\ln\frac{1-\eta_1/\phi}{1-\eta_1/\phi_0}\right)\\ &+2B\frac{\phi}{\phi_0-\phi}\left[\frac{1}{2}\frac{(\eta_1/\phi_0)^2}{(1-\eta_1/\phi_0)^2}-\frac{\phi}{\phi_0-\phi}\frac{\eta_1/\phi_0}{1-\eta_1/\phi_0}+\frac{\phi^2}{(\phi-\phi_0)^2}\ln\frac{1-\eta_1/\phi}{1-\eta_1/\phi_0}\right]\end{aligned} \tag{11}$$

The corresponding expression for the pressure is presented in [9].

At high fluid densities the obtained expressions have two divergences, which appear in $\eta_1 = \phi$ and $\eta_1 = \phi_0$, respectively. Since $\phi < \phi_0$, the first divergence (in $\eta_1 = \phi$) occurs at lower densities than the second one and it leads to the strong overestimation for thermodynamic properties in the region of high densities. It is worth noting that from a physical (or rather geometrical) point of view the divergence should appear near the maximum value of fluid packing fraction, η_1^{max}, available for a fluid in the matrix. This value should be larger than ϕ and smaller than ϕ_0. The divergence in $\eta_1 = \phi$ is connected with the presence of ϕ in the denominator in the last term of eq. 7. The problem appears due to an assumption that the multiplier $1/p_0(R_s)$ introduced in eq. 2 does not depend on the presence of fluid, which is acceptable to some extent and mostly for low and intermediate densities.

It is shown in [14] for a one-dimensional system that the second virial coefficient in the SPT2 approach gives a numerically correct result. For a three-dimensional system it has the following form:

$$B_2 = \frac{4}{3}\pi R_1^3\left[\frac{1}{\phi}+\frac{1+A}{\phi_0}\right] \tag{12}$$

However, with an increase of the fluid density the multiplier $1/\phi$ in eq. 7 should vary and at high densities it will be equal to $1/\eta_1^{max}$. The different corrections for the improvement of SPT2 are proposed in [9,14]. First corrections of the expression 11 for HS fluid in HS and OHS matrices are given in [9], where within SPT2 four different approximations are presented. In the first of them, called SPT2a, the porosity ϕ in eq. 7 is replaced by ϕ_0. As a result, the expression for the chemical potential of an HS fluid in a random matrix is obtained

$$\begin{aligned}\beta(\mu_1^{ex}-\mu_1^0)^{SPT2a} &= -\ln(1-\eta_1/\phi_0)+(1+A)\frac{\eta_1/\phi_0}{1-\eta_1/\phi_0}\\ &+\frac{1}{2}(A+2B)\frac{(\eta_1/\phi_0)^2}{(1-\eta_1/\phi_0)^2}+\frac{2}{3}B\frac{(\eta_1/\phi_0)^3}{(1-\eta_1/\phi_0)^3}\end{aligned} \tag{13}$$

This approximation is not correct, since it does not reproduce the second virial coefficient given in eq. 12.

The second approximation called SPT2b can be derived if ϕ is replaced by ϕ_0 everywhere in the expression of compressibility except the first term on the RHS of eq. 10. And after the corresponding integration of eq. 10 over the fluid density one obtains the expression for the chemical potential as follows:

$$\beta(\mu_1^{ex}-\mu_1^0)^{SPT2b} = -\ln(1-\eta_1/\phi)+(1+A)\frac{\eta_1/\phi_0}{1-\eta_1/\phi_0} + \frac{1}{2}(A+2B)\frac{(\eta_1/\phi_0)^2}{(1-\eta_1/\phi_0)^2}+\frac{2}{3}B\frac{(\eta_1/\phi_0)^3}{(1-\eta_1/\phi_0)^3} \quad (14)$$

Third and fourth approximations, SPT2c and SPT2d, are obtained if ϕ is replaced by ϕ_0 in the third and fourth terms on the RHS of eq. 10 or just in the fourth term on the RHS of eq. 10, respectively. Therefore, the following expressions for the chemical potentials are derived

$$\beta(\mu_1^{ex}-\mu_1^0)^{SPT2c} = -\ln(1-\eta_1/\phi)+(1+A)\frac{\phi}{\phi-\phi_0}\ln\frac{\eta_1/\phi}{1-\eta_1/\phi_0} + \frac{1}{2}(A+2B)\frac{(\eta_1/\phi_0)^2}{(1-\eta_1/\phi_0)^2}+\frac{2}{3}B\frac{(\eta_1/\phi_0)^3}{(1-\eta_1/\phi_0)^3} \quad (15)$$

$$\beta(\mu_1^{ex}-\mu_1^0)^{SPT2d} = -\ln(1-\eta_1/\phi)+(1+A)\frac{\phi}{\phi-\phi_0}\ln\frac{\eta_1/\phi}{1-\eta_1/\phi_0} + (A+2B)\frac{\phi}{\phi-\phi_0}\left[\frac{\eta_1/\phi_0}{1-\eta_1/\phi_0}-\frac{\phi}{\phi-\phi_0}\ln\frac{\eta_1/\phi_0}{1-\eta_1/\phi_0}\right]+\frac{2}{3}B\frac{(\eta_1/\phi_0)^3}{(1-\eta_1/\phi_0)^3} \quad (16)$$

The corresponding expressions for the pressure within the considered approximations are presented in [9]. It should be noted that the approximations SPT2b, SPT2c, and SPT2d give the same second virial coefficient as the original SPT2 approximation in contrast to the SPT2a approximation. Similar to what was done in the one-dimensional case [14] for the high fluid densities to correct the description of thermodynamical properties, we should avoid the problem of divergence, which appears at $\eta_1 = \phi$.

To avoid this divergence the first logarithm in expression 14 is expanded. Such a procedure leads to the new approximation called SPT2b1 [14]:

$$\beta(\mu_1^{ex}-\mu_1^0)^{SPT2b1} = -\ln(1-\eta_1/\phi_0)+(1+A)\frac{\eta_1/\phi_0}{1-\eta_1/\phi_0}+\frac{\eta_1(\phi_0-\phi)}{\phi_0\phi(1-\eta_1/\phi_0)} + \frac{1}{2}(A+2B)\frac{(\eta_1/\phi_0)^2}{(1-\eta_1/\phi_0)^2}+\frac{2}{3}B\frac{(\eta_1/\phi_0)^3}{(1-\eta_1/\phi_0)^3} \quad (17)$$

Two other approximations SPT2b2 and SPT2b3 contain the third type of porosity ϕ^* defined by the maximum value of packing fraction of fluid in porous medium. These approximations provide the more correct description of thermodynamic properties of a fluid in the high-density region. The SPT2b1, SPT2b2, and SPT2b3 approximations similar to other approximations obtained from SPT2 (except SPT2a) reproduce correctly the second virial coefficient presented in eq. 12.

We should also note that in the case when a size of matrix particles, R_0, is essentially larger than a size of fluid particles, R_1, ϕ tends to ϕ_0 and all considered approximations lead to the same result, which is equivalent to a bulk fluid with the effective density $\hat{\eta}_1 = \eta_1/\phi_0$.

COMPUTER SIMULATION DETAILS

In order to assess the theory presented in this study, as well as to estimate an accuracy of the different approximations proposed within the SPT2 approach, the corresponding computer simulations data are required. To this aim, we performed calculations using the GCMC method of [15].

For each of the models of random porous medium and each set of parameters considered in our review the particular matrix configurations are used. During a simulation run a matrix subsystem remains unmovable, e.g., the coordinates of matrix are fixed, while fluid particles can move in a void not occupied by matrix particles. The fluid–matrix and fluid–fluid interactions are of hard core type. The matrices are generated randomly, i.e., the coordinates of matrix particle centers are chosen in the simulation box randomly as well as their orientations if they are of nonspherical shape. Except the case of an HS matrix, configurations of a matrix are formed by using Monte Carlo simulations in a canonical ensemble for a bulk HS system. Since matrices are of a finite size in the simulations, any observable quantity fluctuates depending on a matrix configuration and, hence, an average over matrix configurations should be taken. In the present study, we used 8 matrix configurations for each set of parameters, while the number of matrix particles ranges from 4000 to 10 000. For each simulation run, about 10 000 trial moves per particle are performed, during which the average fluid density is calculated. The average number of fluid particles varies and can be as high as 800 000 depending on the chemical potential and the matrix parameters. We obtained results for fluid density with a statistical error less than 0.5 %, allowing us to make a thorough verification of our theoretical results. To speed up the simulations, the linked cell list algorithm was applied [15].

Therefore, from the simulations we obtained dependencies of the fluid density on the chemical potential, which were compared with the results calculated from the SPT2 approach. The corresponding analysis is made in the next sections for the different models of a fluid in a random porous medium.

HS FLUID IN HS AND OHS MATRICES

According to the formalism presented above, we apply the SPT2 theory for the description of an HS fluid in HS and OHS matrices. We start from concretization of the expressions for the probability of successful insertion of a scaled particle into empty matrices. The corresponding expressions for $p_0(R_s)$ are derived under condition $R_s \le 0$ for the case of HS matrix

$$p_0(R_s) = 1 - \eta_0(1 + R_s/R_0)^3 \tag{18}$$

and OHS matrix

$$p_0(R_s) = \exp\,[-\eta_0(1 + R_s / R_0)^3] \tag{19}$$

respectively, where $\eta_0 = \frac{4}{3}\pi R_0^3\rho_0, \rho_0 = \frac{N_0}{V}$, N_0 is the number of matrix particles, V is the volume of system, R_0 is the radius of matrix particles. Therefore, the geometrical porosity for an HS matrix has a form

$$\phi_0 = p_0(R_s = 0) = 1 - \eta_0 \tag{20}$$

and for an OHS matrix it is

$$\phi_0 = p_0(R_s = 0) = 1 = e^{-\eta_0} \tag{21}$$

Using the SPT theory [9], the following expression for the probe particle porosity, ϕ, is derived

$$\phi = (1-\eta_0)\exp\left[-\left(\frac{3\eta_0\tau}{1-\eta_0} + \frac{3\eta_0(1+\frac{1}{2}\eta_0)\tau^2}{(1-\eta_0)^2} + \frac{\beta\eta_0 P_0}{\rho_0}\tau^3\right)\right] \tag{22}$$

$$\frac{\beta P_0}{\rho_0} = \frac{(1+\eta_0+\eta_0^2)}{(1-\eta_0)^3} \tag{23}$$

in the case of HS matrix and

$$\phi_0 = \exp\left[-\eta_0(1+\tau)^3\right] \tag{24}$$

in the case of OHS matrix, where $\tau = R_1/R_0$ is a size ratio between fluid and matrix particles. It can be easily shown that ϕ is always less than ϕ_0, except the limit of $\tau = 0$, in which $\phi = \phi_0$.

According to eq. 8, the constants A and B are equal to

$$\begin{aligned} A &= 6 + \frac{3\eta_0\tau(\tau+4)}{1-\eta_0} + \frac{9\eta_0^2\tau^2}{(1-\eta_0)^2} \\ B &= \frac{9}{2}\left(1+\frac{\tau\eta_0}{1-\eta_0}\right)^2 \end{aligned} \tag{25}$$

for an HS fluid in an HS matrix and

$$\begin{aligned} A &= 6 + 3\eta_0\tau(\tau+4) + \frac{9}{2}\eta_0^2\tau^2 \\ B &= \frac{9}{2}\left(1+\tau\eta_0\right)^2 \end{aligned} \tag{26}$$

for an HS fluid in an OHS matrix.

Now we estimate the accuracy of the different approximations of SPT2 at various values of $\tau = R_1/R_0$: $\tau = 1$, $\tau = 1/3$, and $\tau = 1/5$. For convenience, we fix the probe particle porosity, ϕ, and it is set at $\phi = 0.35$ in the current section everywhere. It is worth noting that for the HS and OHS models, $\phi = 0.35$ is enough to get a permeable porous medium, i.e., for this value of porosity ϕ the system of pores is over its percolation threshold [18]. A comparison of the approximations SPT2, SPT2a, SPT2b, SPT2c, and SPT2d with the results of GCMC simulations is presented in Fig. 2. It is observed that SPT2a underestimates and SPT2 overestimates the values of chemical potential. The results presented in Fig. 2 show that SPT2b, SPT2c, and SPT2d systematically correct the underestimation of the chemical potential by SPT2a. Also, it is seen that among all approximations, SPT2b gives the most accurate results for the chemical potential in almost all cases in the considered regions of fluid density. Only for the HS matrix with matrix particle sizes equal to the fluid particle sizes ($\tau = 1$), the errors of SPT2b are slightly larger then those of SPT2a. Except in this case the relative errors of SPT2b do not exceed 2 %. The comparison of results obtained in SPT2b and SPT2b1 approximations is presented in Fig. 3. As one can see, SPT2b1 improves the results at intermediate densities, especially for the HS matrix in the case $\tau = 1$. In most cases, the accuracy of SPT2b1 approximation is comparable to the statistical errors of the simulations.

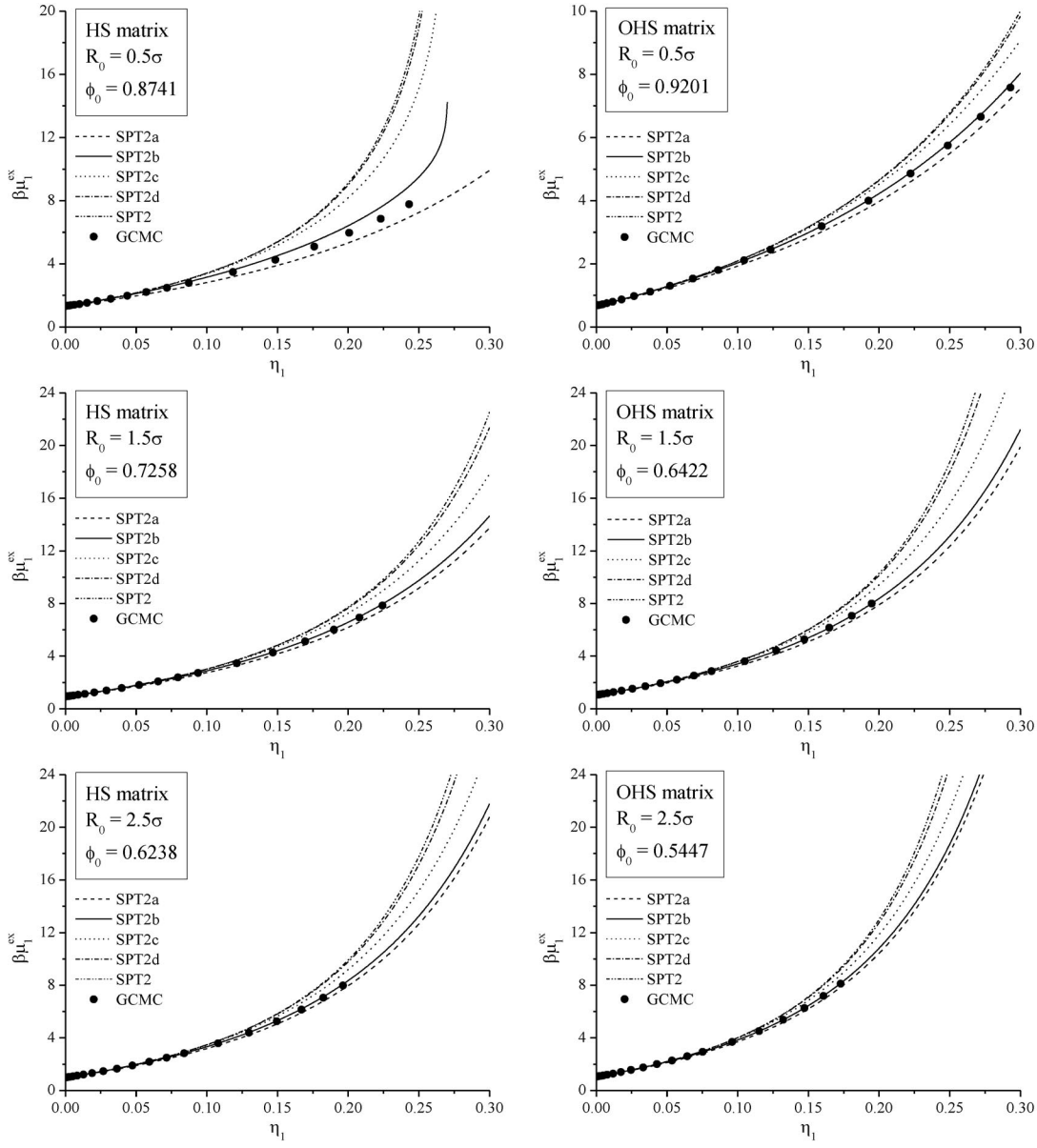

Fig. 2 The excess chemical potential vs. density of a fluid in HS and OHS matrices.

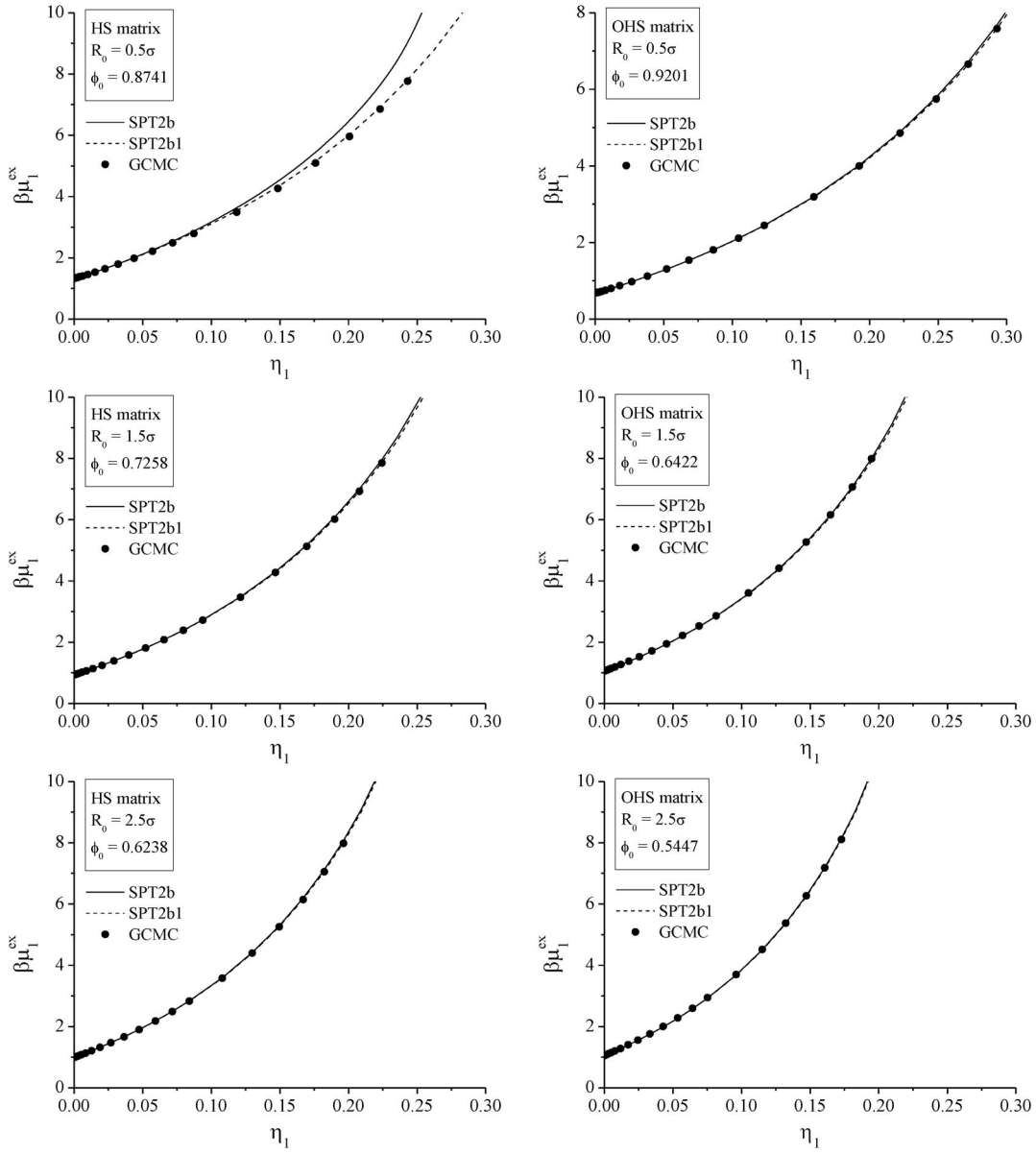

Fig. 3 The excess chemical potential vs. density of a fluid in HS and OHS matrices.

HS FLUID IN SPONGE MATRIX

In this section, we apply the SPT2 theory for the description of HS fluid in a sponge matrix. In contrary to the HS and OHS matrices, where pores present a void free of matrix particles, in a sponge matrix the pores are formed by a volume, which is occupied by matrix particles (see Fig. 1c). Similar to the previous section, we use the general formulation of the SPT2 approach to derive expressions for a particular model of a fluid in a random porous medium. The expression for the probability of successful insertion of scaled particle into an empty sponge matrix, $p_0(R_s)$, is as follows:

$$p_0(R_s) = 1 - \exp\left[-\frac{4}{3}\pi(R_0 - R_s)^3\rho_0\right] = 1 - \exp\left[-\eta_0\left(1 - \frac{R_s}{R_0}\right)^3\right] \tag{27}$$

Therefore, according to eq. 4, the geometrical porosity is

$$\phi_0 = p_0(R_s = 0) = 1 - e^{-\eta_0} \tag{28}$$

and for the probe particle porosity, ϕ, one obtains

$$\phi_0 = p_0(R_s = R_1) = \exp[-\beta\mu_1^0] = 1 - \exp[-\eta_0(1 - \tau)^3], \tag{29}$$

where $\tau = R_1/R_0$.

Using eq. 8, the constants A and B are derived as

$$A = 6 + \frac{12\eta_0\tau e^{-\eta_0}}{\phi_0} + \frac{9\eta_0^2\tau^2 e^{-2\eta_0}}{\phi_0^2} - \frac{3}{2}\eta_0^2\tau^2\frac{1}{\phi_0}(2 - 3\eta_0)e^{-\eta_0}$$
$$B = \frac{9}{2}\left(1 + \frac{\eta_0}{\phi_0}\tau e^{-\eta_0}\right)^2 \tag{30}$$

As a result, within the SPT2 theory the corresponding expressions for the chemical potential of an HS fluid in the different approximations are used (see eqs. 11, 13–17). Since from our previous analysis it is concluded that the SPT2b approximation leads to the best agreement with computer simulations, we restricted ourselves just to this approximation. The accuracy of the SPT2b approximation for the different values of τ is demonstrated in Fig. 4. As in the previous section, we set the probe particle porosity ϕ equal to 0.35 and changed the size of the matrix particles. The same procedure is done for the higher porosity $\phi = 0.50$ (Fig. 4). As one can see, in the considered region of fluid densities the SPT2b gives a satisfactory agreement with the GCMC results, however, a small overestimation is observed in the region of high densities of a fluid. To our best knowledge, for this moment the results presented in our study provide the most accurate theoretical description of the thermodynamic properties of an HS fluid confined in a hard sponge matrix. Moreover, we expect that the approximations SPT2b1, SPT2b2, and SPT2b3 should improve accuracy as it was noticed for the cases of HS and OHS matrices. The detailed analysis of the new approximations for an HS fluid in a hard sponge matrix will be published elsewhere.

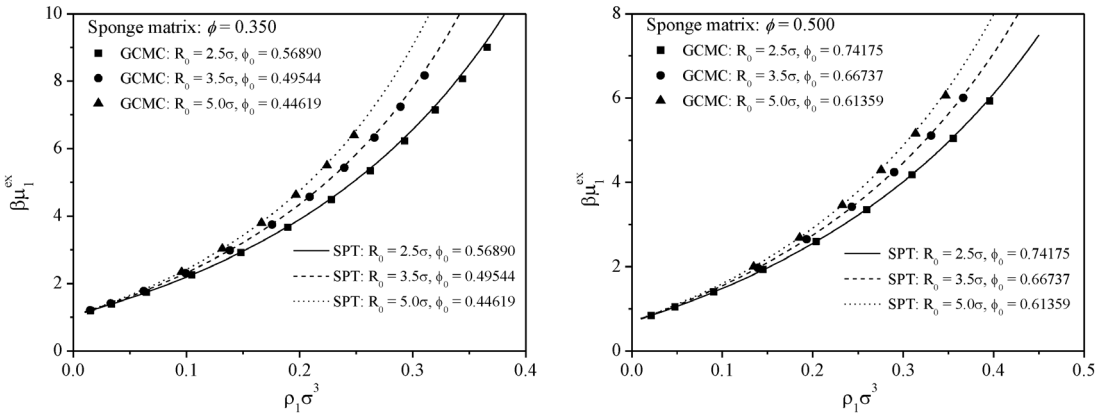

Fig. 4 The excess chemical potential vs. density of a fluid in a sponge matrix of different porosities. Comparison of the SPT2b approximation (lines) with the computer simulations (symbols).

HS FLUID IN HARD CONVEX BODY MATRIX

We introduce a new variation of a model for a random porous matrix, which consists of randomly distributed HCB particles. The main complication in the description of this model, in a comparison with the previous ones, is that the interaction between fluid and matrix particles does not have a spherical symmetry. However, with the use of the SPT theory one can overcome this problem easily. In this section, we present an extension of the SPT2 theory to describe an HS fluid confined in HCB matrix. The matrix convex body particles are characterized by three functional—a volume V_0, a surface area S_0, and the factor $(1/4\pi)$ of the mean curvature R_0. According to this, the corresponding expressions for $p_0(R_s)$ are derived under condition $R_s \le 0$ for the case of an HCB matrix

$$p_0(R_s) = 1 - \eta_0 \left[1 + \frac{S_0}{V_0} R_s + \frac{R_0}{V_0} 4\pi R_s^2 + \frac{1}{V_0} \frac{4}{3} \pi R_s^3 \right] \tag{31}$$

and for an overlapping hard convex body (OHCB) matrix

$$p_0(R_s) = \exp\left[-\eta_0 \left[1 + \frac{S_0}{V_0} R_s + \frac{R_0}{V_0} 4\pi R_s^2 + \frac{1}{V_0} \frac{4}{3} \pi R_s^3 \right] \right] \tag{32}$$

respectively, where $\eta_0 = \rho_0 V_0$ is the packing fraction of matrix particles.

The geometrical porosity for HCB matrix has a form

$$\phi_0 = p_0(R_s = 0) = 1 - \eta_0 \tag{33}$$

and for an OHCB matrix it is

$$\phi_0 = p_0(R_s = 0) = e^{-\eta_0} \tag{34}$$

Using the SPT theory for HCB fluid [19] the following expression for the probe particle porosity ϕ is derived:

$$\phi = e^{-\beta\mu_1^0} = (1-\eta_0) \exp\left[-\left(\frac{3\eta_0\alpha_0\tau}{1-\eta_0} + \frac{3\eta_0\alpha_0\tau^2}{1-\eta_0} \frac{4\pi R_0^2}{S_0} + \frac{9}{2} \frac{\eta_0^2\alpha_0^2\tau^2}{(1-\eta_0)^2} + \frac{\beta P_0 \eta_0 \tau^3}{\rho_0} \frac{4}{3} \frac{\pi R_0^3}{V_0} \right) \right] \tag{35}$$

where

$$\frac{\beta P_0}{\rho_0} = \frac{1}{1-\eta_0} + \frac{3\alpha_0\eta_0}{(1-\eta_0)^2} + \frac{3\alpha_0^2\eta_0^2}{(1-\eta_0)^3}, \quad \alpha_0 = \frac{R_0 S_0}{3V_0}, \tau = R_1 / R_0 \tag{36}$$

in the case of HCB matrix and

$$\phi = \exp\left[-\eta_0 \left(1 + 3\tau\alpha_0 + 3\tau^2\alpha_0 \frac{4\pi R_0^2}{S_0} + \tau^3 \frac{4}{3} \frac{\pi R_0^3}{V_0} \right) \right] \tag{37}$$

in the case of OHCB matrix.

From eq. 8, one obtains the coefficients A and B

$$A = 6 - \frac{3\eta_0\alpha_0\tau}{1-\eta_0}\left(4 + \frac{4\pi R_0^2}{S_0}\tau\right) + \frac{9\eta_0^2\alpha_0^2\tau^2}{(1-\eta_0)^2}$$
$$B = \frac{9}{2}\left(1 + \frac{\tau\eta_0\alpha_0}{1-\eta_0}\right)^2 \tag{38}$$

for an HS fluid in an HCB matrix and

$$A = 6 + 3\eta_0\tau\alpha_0\left(4 + \frac{4\pi R_0^2}{S_0}\tau\right) + \frac{9}{2}\eta_0^2\alpha_0^2\tau^2$$
$$B = \frac{9}{2}\left(1 + \tau\eta_0\alpha_0\right)^2 \tag{39}$$

for an HS fluid in an OHCB matrix.

Using eqs. 31–39 in combination with eqs. 11 and 13–17, we can calculate the chemical potential of an HS fluid confined in HCB or OHCB matrix in all approximations that we proposed. However, for the sake of brevity we skip an analysis of the different approximations and present the results obtained in the best one—the SPT2b approximation (see eq. 14).

To verify the theory, the computer simulations for an HS fluid in OHCB matrix were performed. As an example of OHCB matrix, a system of an HS fluid in a matrix formed by overlapping hard prolate spherocylinders is considered. A length of such spherocylinders is d_0, and a diameter is σ_0. The corresponding effective parameters characterizing a geometry of matrix particles are as follows:

$$R_0 = \frac{1}{4}d_0 + \frac{1}{2}\sigma_0, S_0 = \pi\sigma_0(d_0 + \sigma_0), V_0 = \frac{1}{4}\pi\sigma_0^2\left(d_0 + \frac{2}{3}\sigma_0\right) \tag{40}$$

In the lower panel of Fig. 5, one can see two examples of a system of an HS fluid in OHCB matrix. Upper, the corresponding results for the chemical potential of a confined fluid are presented. It is seen that SPT2b results match perfectly the computer simulation data. Of course, the detailed analysis at higher fluid densities are still required, which will be presented in another paper. Nevertheless, even for these matrix parameters and the ranges of fluid densities it is clear that the SPT2 theory works well for such systems. And also it should be mentioned that there is a possibility to apply the SPT2b1, SPT2b2, and SPT2b3 approximation, which can give better accuracy than the SPT2b approximation.

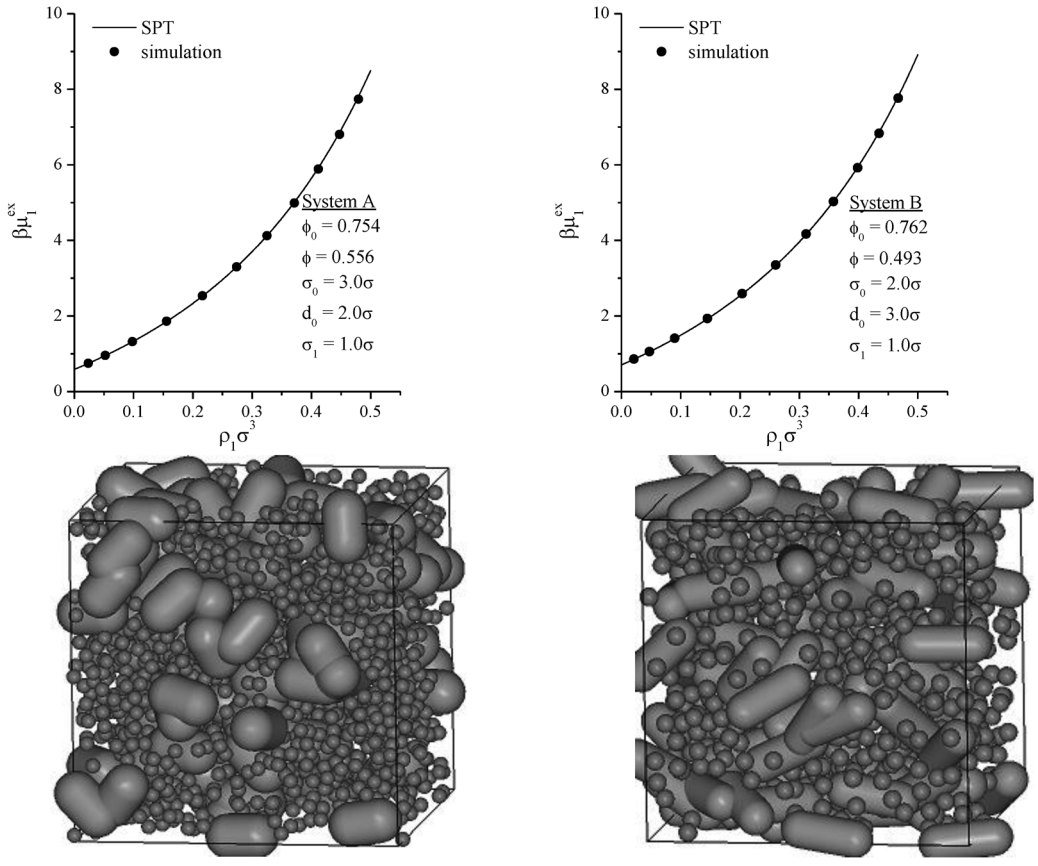

Fig. 5 The excess chemical potential vs. density of a fluid confined in an overlapping hard spherocylinder matrix. Comparison of the SPT2b approximation (lines) with the computer simulations (symbols).

MAPPING BETWEEN THERMODYNAMIC PROPERTIES OF HS FLUID IN DIFFERENT MATRICES

A main idea of the problem considered in this section consists in mapping of thermodynamic properties of a fluid confined in one type of random matrix to its thermodynamic properties in another type of random matrix. It means that we are looking for a possibility to predict the equation of state of a fluid in an arbitrary matrix knowing its equation of state in one certain type of a matrix. In the previous sections we have considered the different models of random porous medium: HS and OHS matrices, sponge matrix, HCB and OHCB matrices. For these models, we propose the rather general SPT2 approach allowing us to obtain analytical results for the thermodynamic properties of a confined fluid. Nevertheless, each of these models needs an additional treatment related to the derivation of porosities ϕ_0 and ϕ, as well as the constants A and B, which are dependent on the probability $p_0(R_s)$ as it is shown in eq. 8. Fortunately, for the given models the expression for $p_0(R_s)$ has been found. However, it is not excluded that one can encounter with some another model of porous medium, for which a derivation of $p_0(R_s)$ is complicated or even not possible to get it at all. In this case the corresponding mapping should be helpful.

All models considered in the present review have only the hard core interaction between fluid particles and walls of porous media. In this context, the geometry of porous medium should be a subject of our interest as a main effect on a fluid, and our task is to relate some of the geometrical (morpho-

logical) peculiarities of porous medium with thermodynamic quantities of a fluid. A morphological approach was proposed in [20,21], in which it was shown that a set of four morphological measures (so-called Minkowski's functionals) is enough to describe efficiently a random porous medium and to predict thermodynamic properties of fluids in porous media. This set of morphological measures includes the porosity ϕ, the pore surface area S, the mean curvature H, and the Gaussian curvature X. Using these morphometric measures, it is shown in [21] that the grand potential can be presented as a linear combination of the pressure P, the planar surface tension σ, and the bending rigidities κ and $\bar{\kappa}$ of a confined fluid:

$$\frac{\Omega}{V} = -P\phi + \sigma s + \kappa h + \bar{\kappa} x \tag{41}$$

where $s = S/V$, $h = H/V$, $x = X/V$, V is the total volume of system. Following this idea, one can conclude that the thermodynamics of an HS fluid depends only on ϕ, s, h, and x. And accordingly, we assume that a fluid has the same thermodynamic properties in any kind of random porous media if it has the same morphometric measures. To verify this assumption we consider two completely different models of a fluid in a random porous medium, and both of them were already mentioned in previous sections as an HS fluid in an OHS matrix and an HS fluid in a sponge matrix. We adjust a density ρ_0 and a size R_0 of matrix particles of OHS matrix to get the equivalent morphometric measures as they are in a sponge matrix. However, due to a lack of the matrix parameters (only two, ρ_0 and R_0), we cannot control all four measures, but the two most important ones, namely, the porosity ϕ and the specific area of pore walls s. The relations for the porosity can be easily derived [18]

$$\phi^{\mathrm{OHS}} = \exp\left(-\frac{4}{3}\pi\rho_0\left(R_{01}^{\mathrm{OHS}}\right)^3\right) \tag{42}$$

$$\phi^{sp} = 1 - \exp\left(-\frac{4}{3}\pi\rho_0\left(R_{01}^{sp}\right)^3\right) \tag{43}$$

for an OHS matrix and a sponge matrix, respectively, where $R_{01}^{\mathrm{OHS}} = R_0 + R_1$ and $R_{01}^{sp} = R_0 - R_1$. It should be noted that, while in the case of OHS matrix a size R_0 is a radius of a matrix particle, in the sponge model R_0 is a radius of cavity (see Fig. 1 and section "HS fluid in sponge matrix"), but for a sake of generality in both cases we use the term "particle". The radii R_{01}^{OHS} and R_{01}^{sp} are introduced for a convenience, and they describe a center–center interaction between fluid and matrix particles.

The specific pore surface area is proportional to $1/R_{01}$ and can be calculated as $s = \partial\phi/\partial R_{01}$. Therefore, the corresponding expressions of the specific pore surface area for an OHS and a sponge matrix are as follows:

$$s^{\mathrm{OHS}} = -\frac{3}{R_{01}^{\mathrm{OHS}}}\phi^{\mathrm{OHS}}\ln\phi^{\mathrm{OHS}} \tag{44}$$

$$s^{sp} = -\frac{3}{R_{01}^{sp}}\left(1-\phi^{sp}\right)\ln\left(1-\phi^{sp}\right) \tag{45}$$

In general, the mean and Gaussian curvatures relate to R_{01} as proportions

$$h \sim 1/R_{01}^2, x \sim 1/R_{01}^3 \tag{46}$$

As mentioned above, there is no possibility to consider these two measures due to a lack of control parameters, thus we have to omit them. On the other hand, one can expect that in our case the curvatures give a relatively small contribution to the thermodynamic properties in a comparison with the contributions of porosity and the pore surface area.

Therefore, the mapping procedure for OHS and sponge matrices consists in the equalities of their porosities and specific pore areas

$$\phi^{\mathrm{OHS}} = \phi^{sp} = \phi,\ s^{\mathrm{OHS}} = s^{sp} \tag{47}$$

From eqs. 42–45 and 47, the corresponding relation between the sizes of matrix particles of the OHS and sponge models can be derived in the form

$$\frac{R_{01}^{\mathrm{OHS}}}{R_{01}^{sp}} = \frac{\phi \ln \phi}{(1-\phi)\ln(1-\phi)} \tag{48}$$

For the particular cases, the numerical correspondence between the sizes of matrix particles obtained from eq. 48 is presented in Table 1. As is seen, we consider a few values of matrix particle sizes at the fixed porosities $\phi = 0.35$ and 0.50. Having ϕ and R_{01}, the matrix densities ρ_0 are calculated from relations 42 and 43. Using the given parameters, a series of GCMC simulations are performed for a fluid in OHS and sponge matrices, and as a consequence the dependencies of chemical potential on fluid density are obtained (Fig. 6). It is observed that the results for both models are nearly identical. A small deviation can be explained by the curvature effects, which are not taken into account in our study. There is a possibility to improve the results by considering OHCB matrix (e.g., a matrix of overlapping spherocylinder particles) instead of OHS matrix, thereby two more control parameters can be introduced and the mean and Gaussian curvatures can be adjusted in such a case.

Table 1 The correspondence between sizes of matrix particles in the model of sponge matrix and the model of OHS matrix.

ϕ	$R_0\sigma$ (sponge)	$R_0\sigma$ (OHS)
0.35	2.500	2.124
	3.500	3.437
0.50	2.500	1.500
	3.500	2.500
	5.000	4.000

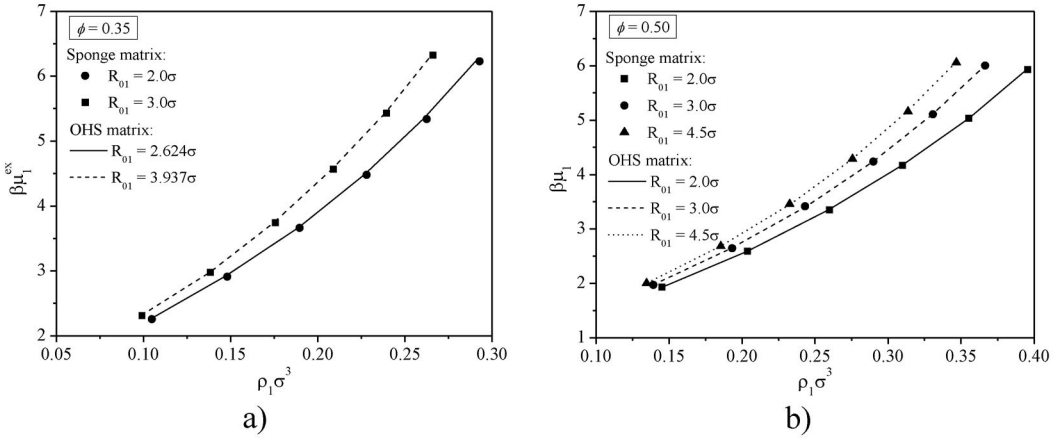

Fig. 6 Mapping between two models of porous medium: sponge matrix and OHS matrix.

THE EXTENSION OF van der WAALS EQUATION OF STATE FOR A SIMPLE FLUID IN RANDOM POROUS MATRICES

It is well established that the short-range order in simple liquids is determined by the repulsive part of interatomic interactions [22,23]. Such a short-range structure is essentially related to the packing of hard core particles, which can be modeled by an HS fluid. The results obtained in our study for an HS fluid in random porous matrices can be used as reference systems in the perturbation theory. As the first step in this direction we look for a possibility to extend the van der Waals equation of state to the case of a simple liquid in a random porous medium. For this purpose, we consider an HS fluid with a fluid–fluid long-range attractive tail in the form of the Kac potential

$$K(r) = \gamma^3 \Phi(\gamma r),\ \Phi(\gamma r) < 0 \tag{49}$$

where r is the interparticle distance. Analogous to the bulk case [24,25], the limit $\gamma \to 0$ leads to the expression for the fluid pressure in the form

$$\frac{\beta P}{\rho_1} = \left(\frac{\beta P}{\rho_1}\right)_{\mathrm{HS}} - 12\beta a \eta_1 \tag{50}$$

The constant a is positive and depends on the pair potential of interaction $K(r)$ as

$$a = -\frac{1}{\sigma^3}\int_0^\infty r^2 dr K(r) \tag{51}$$

where $\sigma = \sigma_1 = 2R_1$ is the diameter of fluid particles.

The term $\left(\frac{\beta P}{\rho_1}\right)_{\mathrm{HS}}$ is a contribution of the reference HS system, and in the SPT2b approximation it is

$$\left(\frac{\beta P}{\rho_1}\right)_{\mathrm{HS}} = -\frac{\phi}{\eta_1}\ln\left(1-\frac{\eta_1}{\phi}\right) + \frac{\phi_0}{\eta_1}\ln\left(1-\frac{\eta_1}{\phi_0}\right) + \frac{1}{1-\eta_1/\phi_0} + \frac{A}{2}\frac{\eta_1/\phi_0}{(1-\eta_1/\phi_0)^2} + \frac{2}{3}B\frac{(\eta_1/\phi_0)^2}{(1-\eta_1/\phi_0)^3} \tag{52}$$

We present an example of the application of the SPT2 approach combined with the van der Waals approximation to the case of attractive fluid confined in an HS matrix. In the reduced units, eq. 50 can be rewritten as

$$P^* = P^*_{\mathrm{HS}} - 2\pi(\rho^*)^2 \tag{53}$$

where $P^* = P\sigma^3/a$ and $\rho^* = \rho_1\sigma^3$. A series of isotherms are calculated using eqs. 52 and 53 for the attractive fluid in an HS matrix of the different porosities and the size of matrix particles. The Maxwell construction is applied to find points for the curves of liquid–vapor coexistence of the systems considered. In Fig. 7 one can see the corresponding phase diagrams in the coordinates $\rho^* - T^*$, where the temperature is used in the reduced units $T^* = k_{\mathrm{B}}T/a$. It is clearly seen from Fig. 7a that the critical temperature and density of a confined fluid is lowering if the matrix porosity decreases. This is the main and well-known effect of confinement caused by an excluded volume. Another effect is considered in Fig. 7b, where the porosity ϕ_0 is fixed, but the size of matrix particles varies in the range $\sigma_0 = 2\sigma - 4\sigma$. One can observe that an increase of the size of matrix particles leads to an increase of the critical temperature of the confined HS fluid. The critical density increases as well in this case. It can be explained by the fact that the pore wall surface area decreases, when a size of matrix particles increases, thus a confinement effects on a fluid become weaker and a fluid behaves more like a bulk fluid, but at the

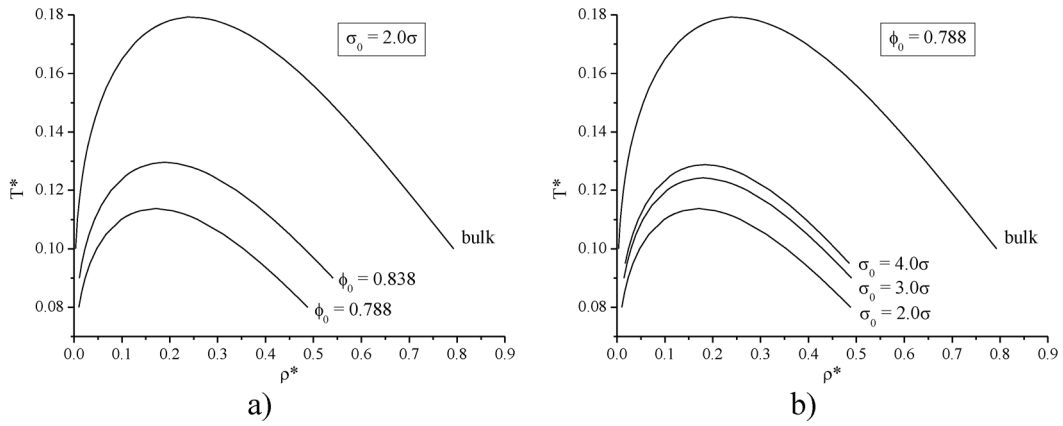

Fig. 7 Liquid–vapor coexistence curves for a fluid in HS matrix of different porosity and different matrix particle sizes.

higher (effective) density. In both cases the phase diagrams become narrower with the critical temperature decreasing and it indicates that the region of liquid–vapor coexistence of confined fluid is getting smaller.

The results obtained in this section are an illustration of the application of our SPT2 results for a description of the reference HS system and how they can be combined with the simplest approach of van der Waals for a study of attractive fluids confined in random porous media.

CONCLUSIONS

In this paper the recently proposed scaled particle theory SPT2 [9] for the description of HS fluid in random porous media is reviewed and applied to the description of thermodynamic properties of an HS fluid in HS and OHS matrices, sponge matrix, and HCB matrix. The developed approaches based on a combination of the exact treatment of a point scaled particle in a system of a HS fluid confined in a matrix and the thermodynamic consideration of a finite-size scaled particle. The obtained analytical expressions for the chemical potential of an HS fluid in a random matrix include two types of porosity. One of them is the geometrical porosity ϕ_0 describing the free void in porous media, and the second one is the probe particle porosity ϕ defined by the adjustable volume for a fluid in porous media and related to the chemical potential of a fluid in the limit of infinite dilution. It is shown that the SPT2 theory describes correctly the second virial coefficient. For an improvement of the SPT2 theory, we have developed several approximations, which lead to the same second virial coefficient predicted earlier by the SPT2 approach. In order to assess these approximations, extensive GCMC simulations were carried out. It is shown that one of them, called SPT2b, has excellent accuracy at small and intermediate fluid densities. The principal defect of the SPT2 and SPT2b approaches is related to the divergence of thermodynamic properties at densities corresponding to the probe particle porosity ($\eta_1 = \phi$). In order to avoid this defect a new approximation called SPT2b1 was proposed. In this approximation the thermodynamic properties have the divergence only at the densities coinciding with the geometrical porosity ($\eta_1 = \phi_0$). This approximation gives the very accurate description at rather high densities with the errors comparable with the computer simulation results for the different parameters of porous media including the case of fluid and matrix particles sizes are equal.

We also discussed the possibilities of mapping the thermodynamic properties of an HS fluid in random porous media of different types. As is shown, the thermodynamic properties of fluid in the different matrices tend to be equivalent if the probe particle porosities and the specific surface pore areas of considered matrices are identical. The obtained results for an HS fluid in random porous media can

be used as a reference system for the description of more realistic fluids. As an example, we considered the extension of the van der Waals equation of state to the case of a simple fluid in random matrices. From the obtained equation, the liquid–vapor coexistence curves were calculated and analyzed. It was shown that with decreasing of porosity the critical temperature and the critical density decrease. It is also observed that at the fixed geometrical porosity ϕ_0, but variable sizes of matrix particles, the critical temperature and the critical density increase if the size of matrix particles becomes larger.

ACKNOWLEDGMENTS

M.H. and T.P. thank the National Academy of Sciences of Ukraine for the support of this work (the joint NASU–RFFR Program). All simulations were performed at the computing cluster of the Institute for Condensed Matter Physics (Lviv).

REFERENCES

1. W. G. Madden, E. D. Glandt. *J. Stat. Phys*. **51**, 537 (1988).
2. J. A. Given, G. Stell. *J. Chem. Phys.* **97**, 4573 (1992).
3. M. L. Rosinberg. "Liquid state methods for disordered system", in: *New Approaches to Problems in Liquid State Theory*, NATO Science series C, Vol. 529, C. Caccamo, J. P. Hansen, G. Stell (Eds.), pp. 245–278, Kluwer, Dordrecht (1999).
4. O. Pizio. "Adsorption in random porous media", in: *Computational Methods in Surface and Colloidal Science* (Surfactant Science Series), Vol. 89, M. Borowko (Ed.), pp. 293–345, Kluwer, Marcel Dekker, New York (2000).
5. A. D. Trokhymchuk, O. Pizio, M. F. Holovko, S. Sokolowski. *J. Phys. Chem.* **100**, 1704 (1996).
6. A. D. Trokhymchuk, O. Pizio, M. F. Holovko, S. Sokolowski. *J. Chem. Phys.* **106**, 200 (1997).
7. M. Holovko, W. Dong. *J. Phys. Chem. B* **113**, 6360 (2009).
8. W. Chen, W. Dong, M. Holovko, X. S. Chen. *J. Phys. Chem. B* **114**, 1225 (2010).
9. T. Patsahan, M. Holovko, W. Dong. *J. Chem. Phys.* **134**, 074503 (2011).
10. H. Reiss, H. L. Frisch, J. L. Lebowitz. *J. Chem. Phys.* **31**, 369 (1959).
11. H. Reiss, H. L. Frisch, E. Helfand, J. L. Lebowitz. *J. Chem. Phys.* **32**, 119 (1960).
12. J. L. Lebowitz, E. Helfand, E. Praestgaard. *J. Chem. Phys.* **43**, 774 (1965).
13. M. F. Holovko, V. I. Shmotolokha, W. Dong. *Condens. Matter Phys*. **13**, 23607 (2010).
14. M. F. Holovko, T. Patsahan, W. Dong. *Condens. Matter Phys.* **15**, 23607 (2012).
15. D. Frenkel, B. Smith. *Understanding Molecular Simulations*, Academic, San Diego (1995).
16. S. L. Zhao, W. Dong, Q. H. Lin. *J. Chem. Phys.* **125**, 244703 (2006).
17. L. A. Fanti, E. D. Glandt. *AIChE J.* **35**, 1883 (1989).
18. S. Torquato. *Random Heterogeneous Materials: Microstructure and Macroscopic Properties*, Springer-Verlag, New York (2002).
19. T. Boublik. *Mol. Phys.* **27**, 1415 (1974).
20. H. Arns, M. A. Knackstedt, K. R. Mecke. "Characterizing the morphology of disordered materials", in: *Morphology of Condensed Matter Physics and Geometry of Spatially Complex Systems*, K. Mecke, D. Stoyan (Eds.), Lecture notes in physics. Springer-Verlag, Berlin (2002).
21. K. R. Mecke, C. H. Arns. *J. Phys. Condens. Matter.* **17**, 503 (2005).
22. J. A. Barker, D. Henderson. *Rev. Mod. Phys.* **48**, 587 (1976).
23. R. Yukhnovskyi, M. F. Holovko. *Statistical Theory of Classical Equilibrium Systems*, Naukova Dumka, Kyiv (1980).
24. M. Kac, G. E. Uhlenbeck, P. C. Hemmer. *J. Math. Phys.* **4**, 216 (1963).
25. J. L. Lebowitz, O. Penrose. *J. Math. Phys.* **7**, 98 (1966).

